

Sawtoothlike de Haas–van Alphen oscillations of a two-dimensional electron system

M. P. Schwarz, M. A. Wilde, S. Groth, D. Grundler, Ch. Heyn, and D. Heitmann
Institute of Applied Physics, University of Hamburg, Jungiusstr. 11, D-20355 Hamburg, Germany
 (Received 14 January 2002; revised manuscript received 9 April 2002; published 14 June 2002)

We present studies on the low-temperature magnetization of a two-dimensional electron system (2DES) in the integer quantum Hall-effect regime. The 2DES was formed in a modulation-doped AlGaAs/GaAs heterostructure. Using molecular-beam epitaxy it has been integrated into a highly sensitive micromechanical cantilever magnetometer. We observe de Haas–van Alphen oscillations at even filling factors up to $\nu=40$ which for $\nu \leq 20$ are almost perfectly sawtoothlike. Oscillations at odd filling factors $\nu=3,5,7$, and 9 are due to the spin splitting of Landau levels. For a quantitative analysis of our data, calculations of the magnetization based on a model density of states (DOS) have been performed. We describe the DOS by narrow Gaussian broadened Landau levels with an energy-independent background. In particular we find that this background DOS increases linearly with ν . This behavior is qualitatively explained using the concept of edge channels. From our data we evaluate the level broadening and, at odd filling factors, the exchange-energy contribution to the spin splitting of Landau levels.

DOI: 10.1103/PhysRevB.65.245315

PACS number(s): 73.43.Fj, 73.20.At, 73.21.Fg, 75.75.+a

I. INTRODUCTION

At low temperature a sawtoothlike de Haas–van Alphen (dHvA) oscillation occurs in the magnetization of a two-dimensional electron system (2DES) whenever the Fermi level crosses a gap in the ground-state energy spectrum. Hence the measurement of this thermodynamic equilibrium quantity is an important source of information about the electronic ground-state properties of the 2DES. A high quality 2DES is favorably realized in an AlGaAs/GaAs heterostructure which is grown with atomic precision by molecular-beam epitaxy (MBE).

Due to the small signal strength of typically less than $2\mu_B^*$ per electron the detection of the dHvA oscillations in a 2DES still represents an experimental challenge. (Here $\mu_B^* = e\hbar/2m^*$ is the effective Bohr magneton, $m^* = 0.067m_e$ the effective electron mass in GaAs.) The first experiments were carried out on fairly large-area samples or multilayered 2DES using a dc superconducting quantum interference device magnetometer¹ or a sensitive torsional magnetometer.² In these studies sinusoidal oscillations with small amplitude were observed. The data have been interpreted with a model density of states (DOS) consisting of Gaussian broadened Landau levels. A large broadening of about $2 \text{ meV} \times \sqrt{B[\text{T}]}$ was assumed, creating a strong overlap between the Landau levels. The oscillations observed in more recent experiments were much closer to a sawtooth.³ In recent studies on samples with extremely high mobility the magnetization was found to be dominated by the electron-electron interaction.^{4,5}

In this paper we report on temperature-dependent magnetization studies on a 2DES which, by MBE growth, has been monolithically integrated into a micromechanical cantilever magnetometer (MCM). The mobility of $\mu = 1.4 \times 10^6 \text{ cm}^2/\text{Vs}$ is high enough to observe dHvA oscillations with a sawtooth profile up to a filling factor $\nu \approx 20$. We compare our experimental data with numerical calculations based on a model density of states (DOS). Like the DOS used by Gornik

*et al.*⁶ this model adds a constant, i.e., energy-independent, background to the Gaussian broadened Landau levels. However, to model our data quantitatively we find that it is crucial to assume this background DOS to increase linearly with the filling factor. We attribute this effect to the influence of edge states. At odd filling factors dHvA oscillations are observed up to $\nu=9$. Here we analyze our experimental data with respect to the enhanced spin splitting of Landau levels.

The paper is organized as follows: In Sec. II we start with a brief description of the theory, then in Sec. III we explain the MCM and the experimental details. In Sec. IV we analyze the effect of disorder and finite temperature on the dHvA oscillations at even filling factors. In Sec. V we focus on the enhancement of spin splitting by electron-electron interaction at odd filling factors. We discuss our results in Sec. VI.

II. THEORY

In the bulk of the 2DES the energy levels of noninteracting electrons subjected to a perpendicular magnetic field B are given by

$$E_j = (j + 1/2)\hbar\omega_c, \quad j = 0, 1, 2, \dots \quad (1)$$

with $\omega_c = eB/m^*$. $N_L = 2N_\nu$ is the level degeneracy with $N_\nu = eB/h$, $\nu = n_s/N_\nu$ the filling factor and n_s the carrier density. Without disorder the resulting DOS can be expressed as

$$D(E) = N_L \sum_{j=0}^{\infty} \delta(E - E_j). \quad (2)$$

In thermal equilibrium the Fermi-Dirac distribution,

$$f(E, \chi, T) = \left[1 + \exp\left(\frac{E - \chi}{kT}\right) \right]^{-1}, \quad (3)$$

determines the occupation of the levels. With this, the electrochemical potential χ , free energy F , and magnetization M

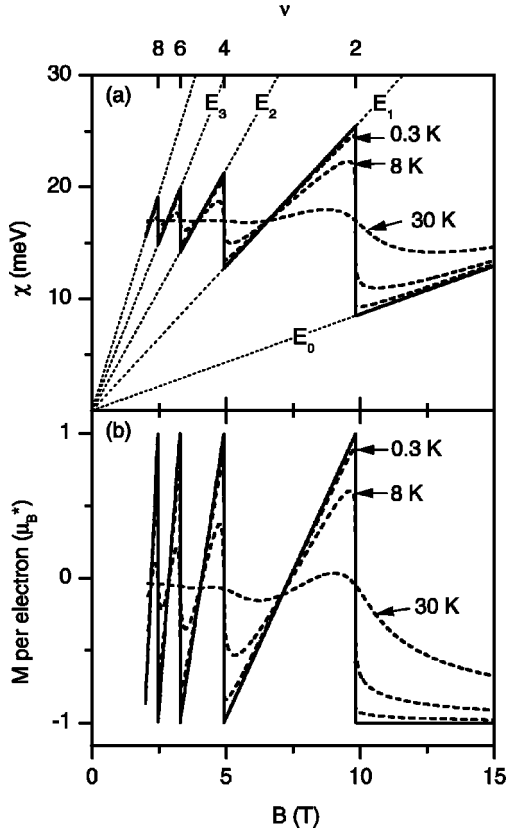


FIG. 1. (a) Calculated chemical potential χ and (b) magnetization M of a 2DES with $n_s = 4.75 \times 10^{11} \text{ cm}^{-2}$. The results for the ideal system at $T=0$ are shown as solid lines. The dotted lines in (a) are the Landau energies $E_j = (j+1/2)\hbar\omega_c$ for $j=0, \dots, 4$. The dashed lines in (a) and (b) show the results if we assume Gaussian broadened Landau levels with $\Gamma=0.29 \text{ meV}$ at finite temperatures $T=0.3, 8, 30 \text{ K}$.

at fixed particle number $N = n_s A$ (A is the 2DES area) can be calculated from the DOS using

$$n_s = \int f(E, \chi) D(E) dE, \quad (4)$$

$$F = \chi N - kTA \int D(E) \ln \left[1 + \exp\left(\frac{\chi - E}{kT}\right) \right] dE, \quad (5)$$

$$M = - \left. \frac{\partial F}{\partial B} \right|_{N, T}. \quad (6)$$

The magnetization and chemical potential for an ideal 2DES at $T=0 \text{ K}$ according to Eqs. (4)–(6) are shown as solid lines in Fig. 1. Both M and χ are oscillating functions of the magnetic field. At even filling factor the chemical potential jumps discontinuously between two adjacent Landau levels with separation $\Delta\chi = \hbar\omega_c = 2\mu_B^* B$. The discontinuities of the magnetization curve ΔM are related to the oscillation of χ via the Maxwell relation $(\partial M / \partial \chi)|_B = (\partial N / \partial B)|_\chi$ which in our case can be simplified to

$$\frac{\Delta M}{N} = \frac{\Delta\chi}{B}, \quad (7)$$

which means the amplitude is $\Delta M = 2\mu_B^*$ per electron, independent of the magnetic field. In Secs. IV and V we will use relation (7) to determine the effective energy gap $\Delta E = \Delta\chi$ in the ground-state energy spectrum. At finite temperature the smearing of the Fermi-Dirac distribution reduces the oscillation amplitude and the discontinuities in χ and M are smoothed.

As we will show later, our experimental results are well described by the model DOS given by

$$D(E) = xD_0 + (1-x)N_L \sum_j \frac{1}{\sqrt{2\pi}\Gamma} \exp\left[-\frac{(E-E_j)^2}{2\Gamma^2}\right]. \quad (8)$$

In this particular model DOS the sample disorder is accounted for by assuming a Gaussian broadening of the Landau levels. The phenomenological approach of adding a constant, i.e., energy-independent, fraction x of the zero-field DOS $D_0 = m^*/\pi\hbar^2$ as a background has been applied before to model the observations of earlier experiments on thermodynamic quantities.^{1,6} The magnetization and chemical potential at finite temperature calculated for Gaussian broadened Landau levels are plotted as dashed lines in Fig. 1.

III. EXPERIMENT

The 2DES was integrated into a GaAs cantilever which is metallized from the backside. It is placed close to a metallic ground plane, forming a capacitor (see inset of Fig. 2). The fabrication and characteristics of such a device have been described previously.⁷

The MCM is sensitive to the torque,

$$\vec{\tau} = \vec{M} \times \vec{B}_{\text{total}}, \quad (9)$$

acting on the magnetization \vec{M} of the 2DES in an external magnetic field \vec{B}_{total} . In our experiment the normal of the 2DES is tilted by an angle of 15° with respect to the direction of the external field. The torque deflects the cantilever from its equilibrium position resulting in a change of capacitance ΔC , which is measured using a highly sensitive capacitance bridge. For small deflections the relation between τ and ΔC is linear:

$$\tau = K \Delta C. \quad (10)$$

To calibrate the sensor we determine K by applying a dc voltage between the cantilever and ground plane and measure the change in capacitance due to the resulting electrostatic force.⁷ For the particular device used in this study we find $K = 1.39 \times 10^{-8} \text{ Nm/pF}$, independent of the temperature from 0.3 to 30 K. This allows us to detect torques as small as $1 \times 10^{-14} \text{ Nm}$ which, at a field of 10 T, corresponds to a magnetic moment of $3 \times 10^{-15} \text{ J/T}$. The total area of the 2DES used in the experiment was 1.28 mm^2 . The MCM device was mounted on the cold finger of a vacuum loading

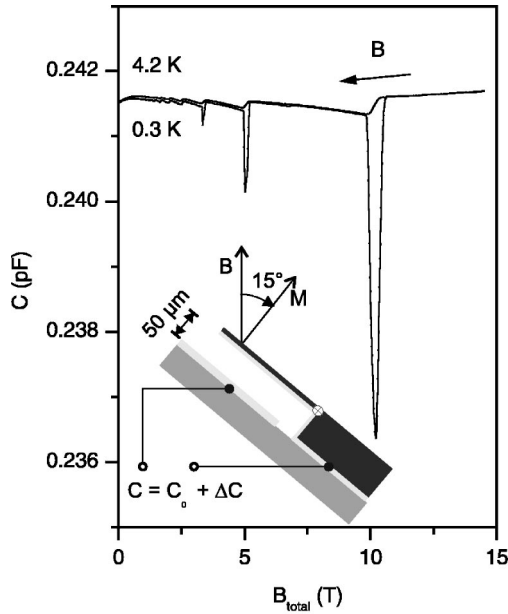


FIG. 2. Raw experimental data at $T=0.3$ K and $T=4.2$ K. The total magnetic field was swept at 0.2 T/min from 14.5 to 0 T. The downward peaks in the low-temperature curve are due to eddy currents. Due to the geometry used in the experiment a positive magnetization signal causes the change in capacitance to be negative. The inset schematically shows the experimental setup. The cantilever is metallized from the backside and mounted on a sapphire substrate. The capacitance $C = C_0 + \Delta C$ is measured with respect to a metallic ground plane on the sapphire substrate. The distance between cantilever and ground plane is $d \approx 50$ μm .

^3He refrigerator providing a minimum base temperature of 0.3 K. The sample temperature was controlled via a calibrated thermometer on the ^3He -cooling stage. A second resistance thermometer was placed close to the sample to ensure thermal equilibrium.

The magnetization measurements presented here were performed after illumination with a light emitting diode. The electron mobility estimated from magnetotransport on Hall bar samples prepared from the same wafer is $\mu = 1.4 \times 10^{-6}$ cm^2/Vs at a carrier density $n_s = 4.75 \times 10^{11}$ cm^{-2} . Experimental data were taken by recording the capacitance signal while sweeping the magnetic field at a rate of 0.2 T/min (Fig. 2). Two features have to be distinguished: the sharp oscillations due to the dHvA effect and the peaklike structures originating from eddy currents induced by the sweeping magnetic field.^{8,9} Additional background signals due to the bulk material of our device are small.

A set of experimental magnetization curves, taken at temperatures from 0.3 to 30 K, is shown in Fig. 3. To remove the small monotonous background signal at low magnetic field a second-order polynomial in $1/B$ was fitted to the original magnetization data at $T=30$ K and subtracted from all curves. At $T=0.3$ K dHvA oscillations are resolved for magnetic fields $B > 0.5$ T. They become washed out with increasing temperature. The upward spikes occurring in the low-temperature curves at small integer filling factors are due to the eddy currents. They reverse their polarity when

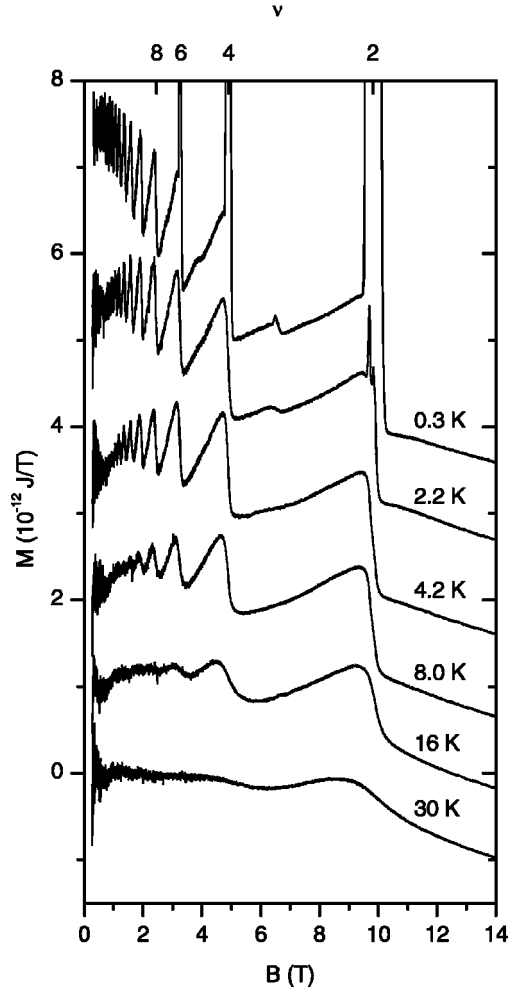


FIG. 3. Experimental magnetization curves as a function of the magnetic field perpendicular to the 2D plane. A second-order polynomial in $1/B$ fitted to the low-field part of the 30 K has been subtracted from the original experimental data. The curves have been offset for clarity. For $T \leq 2.2$ K peaks due to eddy currents are superimposed to the dHvA oscillations. The carrier density determined from the $1/B$ oscillation period is $n_s = 4.75 \times 10^{11}$ cm^{-2} .

changing the sweep direction of the magnetic field and can thus be clearly distinguished from the equilibrium dHvA signal.

IV. de HAAS-VAN ALPHEN EFFECT AT EVEN FILLING FACTORS

We first focus on the dHvA oscillations at even filling factors. At the minimum experimental temperature of $T = 0.3$ K the onset of oscillations is at $B = 0.5$ T, corresponding to a filling factor $\nu = 40$. For magnetic fields $B \geq 1$ T, i.e., $\nu \leq 20$, the oscillations become almost perfectly sawtoothlike. At $B \geq 10.5$ T, i.e., for $\nu < 2$, $M(B)$ varies monotonously with a small negative slope (Fig. 3).

The peak-to-peak amplitude ΔM at even filling factors increases as a function of magnetic field B . A maximum value of $\Delta M \approx 2\mu_B^* N$ is reached in the limit of high fields at $\nu = 2$. In Fig. 4 we have calculated the effective energy gap

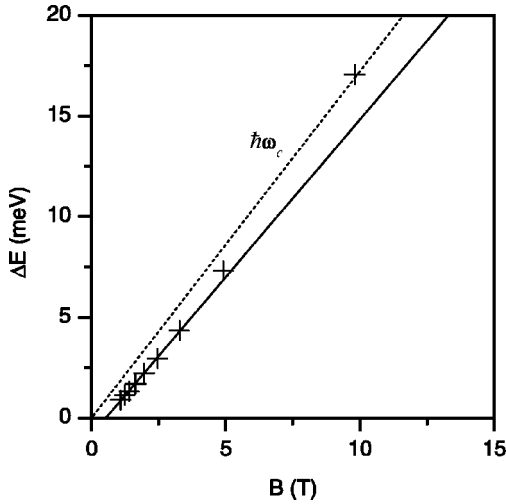


FIG. 4. Effective energy gap ΔE at even integer filling factor (evaluated from the magnetization at $T=0.3$ K). The solid line is a linear fit to the data with $\nu \geq 4$. The dashed line represents the cyclotron energy $\hbar\omega_c$.

ΔE from the experimental values of ΔM at $T=0.3$ K according to Eq. (7). The linear extrapolation of the data to $B=0$ intersects the B axis at a finite value, indicating that the effective energy gap collapses at finite B . This is attributed to a finite level width due to disorder.

While changing from the local maximum to its local minimum at an even integer filling factor the dHvA oscillation exhibits a finite slope. In this small interval ΔB the magnetization varies almost linearly with B . This is attributed to a finite number of states between the Landau levels. To estimate their amount we follow the recent approach of Wieggers *et al.* and evaluate $\Delta B/B_\nu$, where B_ν is the magnetic field corresponding to the even integer filling factor ν .³ The number of states that the Fermi level crosses is

$$n_g = \nu \Delta N_L = \nu \frac{e \Delta B}{h} = n_s \frac{\Delta B}{B_\nu}. \quad (11)$$

Thus $\Delta B/B_\nu = n_g/n_s$ is a measure for the relative number of states between the Landau levels. We find a slight decrease of this quantity from 6% at $\nu=2$ to 3% at $\nu=26$. [Fig. 5(a)]. Using the effective energy gaps from Fig. 4 we can now obtain an estimate of the average DOS at the Fermi level D_g in the interval ΔB , i.e., the value of the DOS between the highest occupied and the lowest unoccupied Landau level:

$$D_g = n_g / \Delta E. \quad (12)$$

The result is shown in Fig. 5(b). We find D_g/D_0 to increase linearly with the filling factor from 6% at $\nu=2$ to 67% at $\nu=18$, which corresponds to a slope of 3.8×10^{-2} .

The temperature dependence of the oscillation amplitude at even filling factors is shown in Fig. 6 for $\nu=2$ to $\nu=8$. At $\nu=2$ we find a smooth, almost linear decrease of ΔM between 0.3 and 30 K. At higher filling factor the temperature dependence becomes steeper.

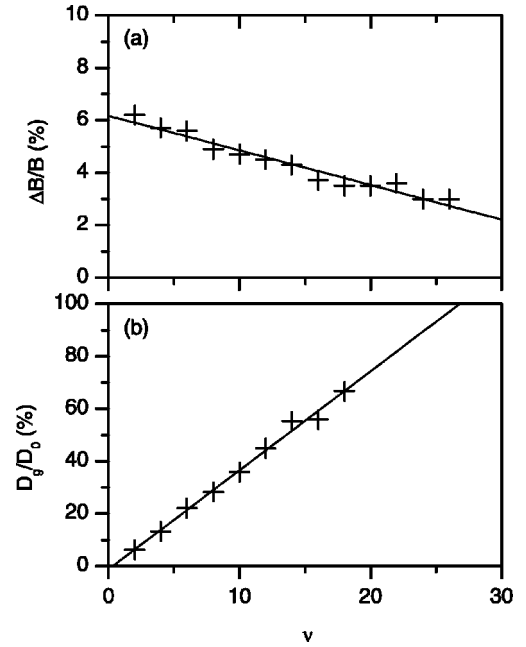


FIG. 5. (a) $\Delta B/B_\nu$, (b) average DOS at the Fermi level at even filling factor. The solid lines are linear fits to the data.

We first compare our experimental data with the temperature dependence expected from the Lifshitz-Kosevich formula:¹⁰

$$M(T) = M_0 \frac{x}{\sinh x}, \quad x = \frac{\pi^2 k T}{\mu_B^* B}. \quad (13)$$

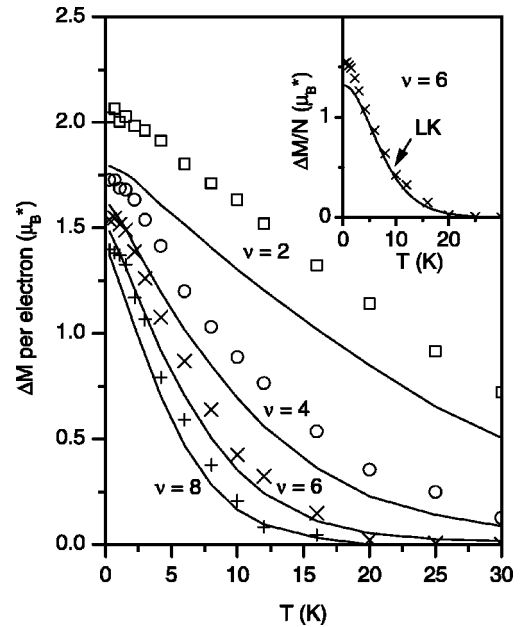


FIG. 6. Temperature dependence of the oscillation amplitude at even filling factors. The experimental values are indicated by symbols, the model calculation as solid lines. In the inset the experimental data at $\nu=6$ are compared to the Lifshitz-Kosevich formula (solid line denoted by LK).

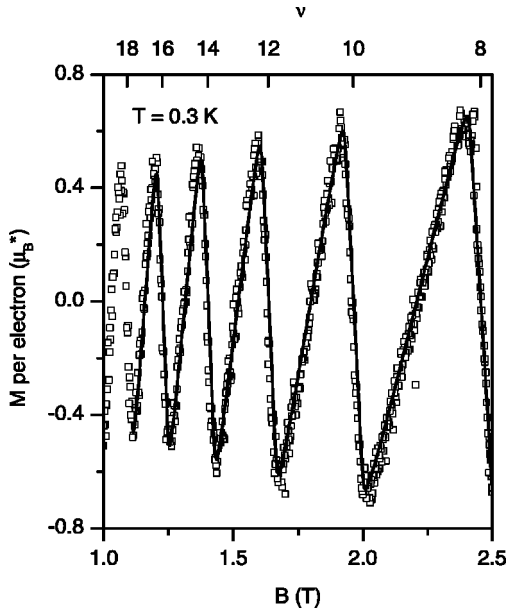


FIG. 7. Comparison of experimental magnetization with the model calculation. To extract the oscillating part of the measured magnetization a smooth background has been subtracted from the data. The solid line represents the result of the model calculation. The parameters for the calculation were $\Gamma = 0.08 \text{ meV}/\sqrt{B[\text{T}]}$ and $b = 2.3 \times 10^{-2}$.

This analytical expression, which is usually applied to describe the dHvA effect in three-dimensional (3D) metals and 2D organic metals, is a good approximation to the relative temperature dependence in the limit of high temperature and large filling factors. For $\nu = 6$ the experimental data and the Lifshitz-Kosevich formula are plotted in the inset of Fig. 6. Here M_0 was adjusted to fit the experimental data points at high temperature. The analytical expression deviates from the experimental data at $T < 3 \text{ K}$. For $\nu \leq 4$ we find that Eq. (13) is not applicable to describe the observed temperature dependence even at high temperature.

To perform a more detailed and, in particular, quantitative analysis we have calculated the magnetization numerically using the model DOS given by Eqs. (8) and (4)–(6). In order to account for the linear increase of D_g found in the experiment (Fig. 5) it is crucial to assume the background density $x D_0$ to be proportional to the filling factor by setting $x = b\nu$. Calculations have been performed using either a magnetic-field independent level-broadening parameter Γ or a Γ proportional to $B^{1/2}$. For a background DOS of $b = 2.3 \times 10^{-2}$ and $\Gamma = 0.08 \text{ meV} \times \sqrt{B[\text{T}]}$ we find a very good agreement with our experimental data. For comparison both calculated and experimental magnetization between 1 and 2.5 T are plotted in Fig. 7. In this regime the model calculation with the $B^{1/2}$ dependence of Γ reproduces our data within the experimental accuracy. The assumption of a magnetic-field independent Γ cannot explain our results.

The solid lines in Fig. 6 denote the numerically calculated temperature dependencies. They match the experimental data for $\nu \geq 6$. At $\nu = 2$ and $\nu = 4$ the calculated values are systematically smaller than the experimental, but the relative scaling is reproduced.

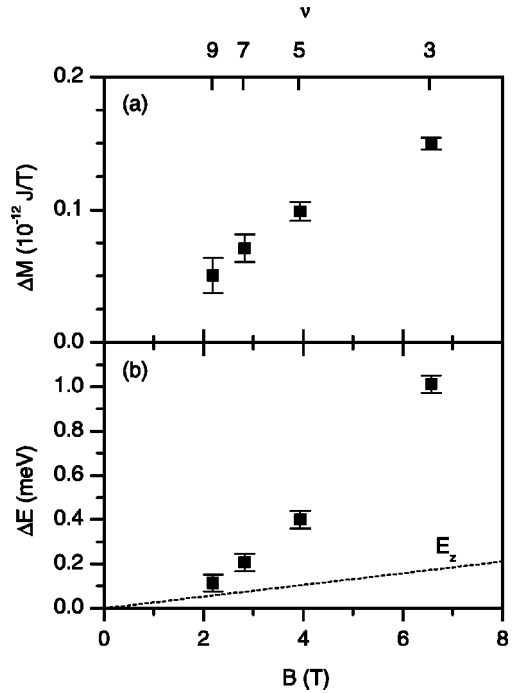


FIG. 8. (a) Oscillation amplitude and (b) effective energy gap at odd filling factor. The dashed line in (b) represents the bare Zeeman energy.

V. de HAAS–VAN ALPHEN EFFECT AT ODD FILLING FACTORS: ENHANCED SPIN SPLITTING

At low temperature dHvA oscillations at odd filling factors are observed for $\nu \leq 9$. The oscillation amplitudes ΔM at $T = 0.3 \text{ K}$ are shown in Fig. 8(a) as a function of magnetic field. In Fig. 8(b) the effective energy gap at odd integer filling factor has been calculated from ΔM according to Eq. (7). It is enhanced with respect to the bare Zeeman energy,

$$E_z = |g| \mu_B B_{total}. \quad (14)$$

Here μ_B is the spin Bohr magneton and $g = -0.44$ for electrons in GaAs.

In order to model the features observed in the magnetization at odd filling factors we have extended the DOS model by introducing the spin splitting of the Landau levels according to

$$E_{j,\sigma} = (j + 1/2) \hbar \omega_c + \sigma g^* \mu_B B, \quad (15)$$

with $j = 0, 1, 2, \dots$ and $\sigma = \pm 1/2$ for the spin quantum number. The effective g factor g^* is used to parametrize the magnitude of spin splitting. The experimental data and calculated traces around $\nu = 3$ are compared in Fig. 9. The agreement is rather satisfactory. The parameters used for Fig. 9(b) were $g^* = 5$ and $\Gamma = 0.15 \text{ meV}$. The linear increase of the magnetization between $\nu = 4$ and $\nu = 2$ has been subtracted in order to visualize the oscillation at $\nu = 3$.

The experimental value for $\Delta B/B$ is 9.5% at $\nu = 3$ and 8.1% at $\nu = 5$. Estimating the average DOS D_g between the Landau levels according to Eq. (12) we find $D_g = 1.5 D_0$ at $\nu = 3$ and $3.4 D_0$ at $\nu = 5$.

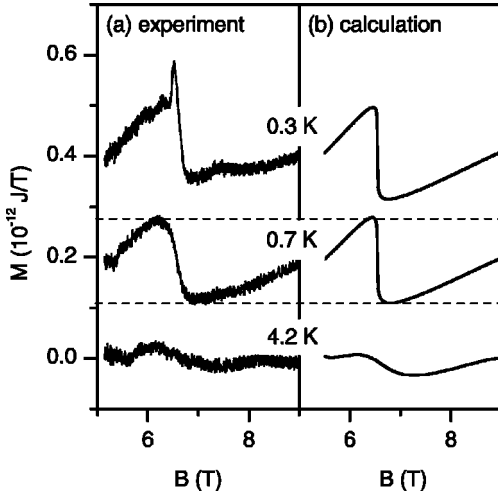


FIG. 9. (a) Experimental magnetization and (b) the result of the model calculation at $\nu=3$. For the calculation $g^*=5$ and $\Gamma=0.15$ meV has been used. A linear function corresponding to the increase in the magnetization between $\nu=4$ and $\nu=2$ has been subtracted from the curves. The peak in the 0.3 K measurement is due to eddy currents. At $T=0.3$ K a shoulder at 7.8 T (indicated by an arrow) seems to reduce the measured amplitude.

The temperature dependence of the peak-to-peak amplitudes at $\nu=3$ and $\nu=5$ is shown in Fig. 10. The suppression of the oscillation with increasing temperature is strong compared to even filling factors in this field range. The dependence from the model calculation for $\nu=3$ is shown as a solid line.

A g^* factor larger than the bare value of $|g|=0.44$ in GaAs is well known from magnetotransport studies and is attributed to the Coulomb-exchange interaction.¹¹ Its relevant energy scale is the Coulomb energy

$$E_C = \frac{e^2}{4\pi\epsilon\epsilon_0 l_B}, \quad (16)$$

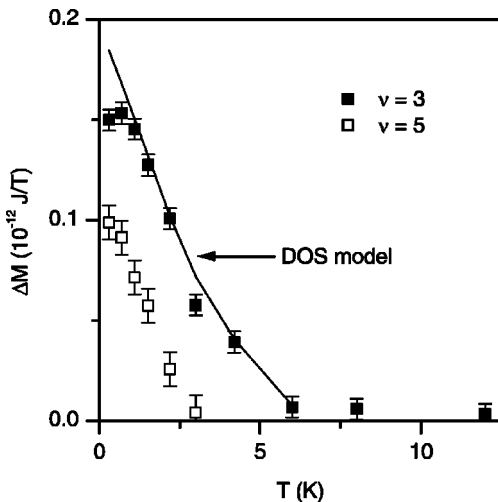


FIG. 10. Temperature dependence of the oscillation amplitude at $\nu=3$ (■) and $\nu=5$ (□). The result of the model calculation at $\nu=3$ is shown as a solid line. The energy separation of the spin sublevels was assumed to be $\Delta E = g^* \mu_B B_{total}$ with $g^*=5$.

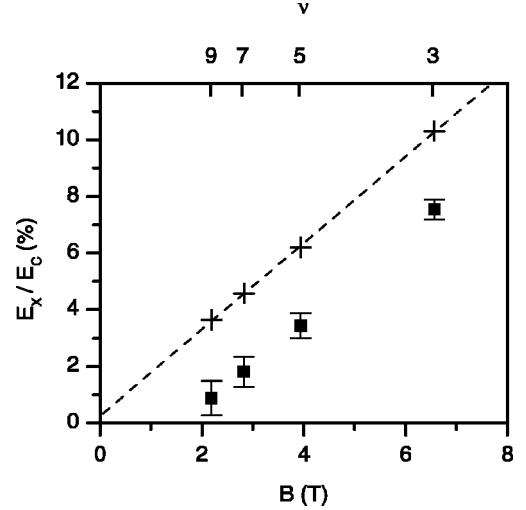


FIG. 11. Exchange-energy contribution E_x at odd filling factors in units of the Coulomb energy E_C . The solid symbols give the bare value of $(\Delta MB - |g| \mu_B B_{total})/E_C$. The crosses give the value which has been corrected for the effect of level broadening according to Eq. (17). The dashed line is a linear fit.

where $\epsilon=12.9$ is the static dielectric constant of GaAs and $l_B = (\hbar/eB)^{1/2}$ is the magnetic length. In the following we explicitly evaluate the exchange-energy contribution E_x to the experimentally observed spin splitting energy ΔMB from the relation

$$\Delta MB + 2\Gamma = g^* \mu_B B = |g| \mu_B B + E_x, \quad (17)$$

where Γ accounts for the level broadening. We take $\Gamma = 0.06$ meV $\times \sqrt{B[\text{T}]}$, which reproduces the result of $\Gamma = 0.15$ meV at $B = 6.55$ T. In Fig. 11 the ratio E_x/E_C is plotted as a function of magnetic field. The linear increase with magnetic field implies that the ratio E_x/E_C is proportional to the spin polarization

$$\frac{N_\uparrow - N_\downarrow}{N_\uparrow + N_\downarrow} = \frac{1}{\nu} \alpha B. \quad (18)$$

VI. DISCUSSION

Due to the high precision of our measurement we are able to analyze the detailed shape of the dHvA oscillation for a large range of filling factors. Especially we find that the DOS between Landau levels increases linearly with the filling factor. The background DOS is crucial to explain the almost linear decrease of the magnetization which occurs in a magnetic-field interval around an even integer filling factor. This finite slope is different from the case of an ideal 2DES, where a discontinuous jump is expected. Also it cannot be explained simply by overlapping broad Landau levels or smearing of the Fermi level due to finite temperature. These effects would both cause a strong curvature in the shape of the dHvA oscillation.

Several theoretical approaches have addressed the issue of a finite value of the DOS between Landau levels. One is the statistical model for inhomogeneities proposed by Gerhardt's

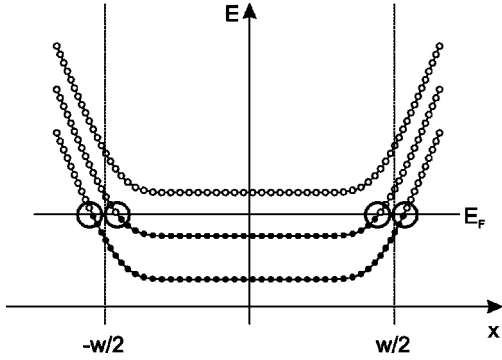


FIG. 12. Edge-state formation at the sample boundary according to Ref. 17. Electron states are filled up to the Fermi level E_F . The positions of edge channels are emphasized by black circles, w denotes the sample width.

et al. which they have used to describe the features observed in earlier magnetization measurements.^{12,13} A large value of the DOS between Landau levels is also predicted for disorder having a finite correlation length.¹⁴ Calculations taking into account the effect of self-consistent screening suggest the level width to be an oscillating function of the filling factor. The effect of screening on the magnetization of a very high-mobility 2DES have been considered by Meinel *et al.*⁵ However, in these theoretical studies no special attention has been paid to the magnetic-field and filling-factor dependence of the value of the DOS between Landau levels. Assuming a spatially correlated random potential a strong decrease of the DOS between Landau levels with magnetic field has been predicted.¹⁵ This behavior is in qualitative agreement with our observation. Recently Itskovsky *et al.* have discussed the exact wave form of the dHvA oscillations in a two-dimensional metal. Here, a finite slope of the magnetization around integer filling factors is due to equilibrium transfer of electrons to a reservoir with field-independent energy spectrum.¹⁶

We would like to propose that the experimental result of a background DOS that increases linearly with the filling factor reflects directly the contribution from the edge states. It is a well established picture that edge states play a crucial role to the properties of a 2DES in the quantum Hall-effect regime.¹⁷ Calculations of the magnetization of a finite-size 2DES (Ref. 18 and 19) have revealed a finite slope of the dHvA oscillation at integer filling factor, even without any disorder. This finite slope is attributed to the presence of edge states. Intuitively one can identify these edge states with the states forming the DOS between the bulk Landau levels in our model: At integer filling factor the number of states at the Fermi level becomes very small in the bulk of the sample; due to the confining potential at the edge of a finite 2DES the Landau levels are bent upward, intersect the Fermi level, and form one-dimensional channels (see Fig. 12).

In a more microscopic model including electrostatic interaction alternating compressible and incompressible stripes form at the sample edge.²⁰ In thermal equilibrium persistent currents with alternating direction are predicted to flow in these stripes.²¹ The effect of these persistent currents on the

equilibrium magnetization has been considered by Bremme *et al.*²² In our experiment it is not possible to exactly distinguish the different contributions from edge and bulk to the total magnetic moment of the sample. However, identifying the states forming the background DOS with the states forming the edge channels one may estimate the fraction of the 2DES area which is effectively covered by the edge channels. In this picture if each edge channel gives rise to the same contribution to the DOS the linear increase of the background DOS is simply due to the increase in the number of channels. Assuming the edge channel at $\nu=2$ to be a single stripe at the boundary of the 2DES mesa which covers 6% of the sample area, we can estimate a width of 16 μm for this channel. This seems to be rather large if compared to the theoretical estimates of Ref. 20 and recent experimental results,²³ suggesting that in our sample the disorder potential causes states with similar properties to form also in the interior of the 2DES.

We now discuss the broadening of the Landau levels. This parameter is determined by the curvature at the tips of the sawtooth and the overall dependence of the amplitude on the magnetic field. Compared to previous studies the value of $\Gamma = 0.08 \text{ meV} \times \sqrt{B[\text{T}]}$ extracted from our model calculation is very small, as intuitively expected from the experimentally observed very sharp sawtooth. The theory by Ando *et al.* predicts semielliptical Landau levels with a width determined by the zero-field mobility of the 2DES:²⁴

$$\Gamma = \frac{\hbar e}{m^*} \sqrt{\frac{2}{\pi \mu}} B. \quad (19)$$

Using our zero-field mobility of $\mu = 1.4 \times 10^6 \text{ cm}^2/\text{Vs}$ we get $\Gamma = 0.12 \text{ meV} \times \sqrt{B[\text{T}]}$. On the one hand this value is in good agreement with the result of our model calculation. On the other hand our model uses Gaussian level broadening which is predicted by different approximations to the scattering process.^{15,25,26} However, with such a small level width, the experimental data do not allow us to distinguish between different models for the exact shape of a Landau level.

The enhanced spin splitting of the Landau levels observed at odd filling factors is caused by electron-electron interaction. A maximum enlargement of the effective energy gap due to Coulomb-exchange interaction is found at $\nu=3$. Here the comparison with the model calculation suggests an effective Landé factor of $g^*=5$. In Fig. 11 we have explicitly derived the exchange energy contribution E_x to the enhanced g^* factor. As predicted by Ando and Uemura,²⁷ we find E_x to be proportional to the Coulomb energy E_C and the spin population difference:

$$E_x = \alpha E_C \frac{N_{\uparrow} - N_{\downarrow}}{N_{\uparrow} + N_{\downarrow}}. \quad (20)$$

The value of $\alpha = 0.3$ for our sample means that the contribution due to electron-electron interaction is about 30% of the Coulomb energy times the spin population difference. A maximum contribution of $\alpha = (\pi/2)^{1/2}$ is predicted for $\nu=1$ by Kallin and Halperin for an ideal 2DES.²⁸ The experimen-

tally observed reduction of this value can be attributed to disorder and a finite thickness of the 2DES.

It has been predicted theoretically that interactions renormalize not only the spin level but also the Landau-level energies, causing an enhancement of the dHvA amplitude at even filling factors. In our sample the dHvA amplitude at $\nu = 2$ is, in spite of the disorder apparently reducing ΔM , about $2\mu_B^*$ per electron which is the theoretically predicted value for noninteracting electrons without disorder. Our model calculation, which neglects the electron-electron interaction, successfully describes the effect of disorder and finite temperature for filling factors $\nu \geq 6$. In case of $\nu = 2$ and $\nu = 4$ the calculated oscillation amplitudes are systematically smaller than in the experiment (Fig. 6). Calculations by MacDonald *et al.* have revealed a very similar behavior: The disorder reduces the dHvA oscillation amplitude at $\nu = 2$ to about $1.5\mu_B^*$. However, including the effect of interaction in the Hartree-Fock approximation restores the amplitude to a value of about $2.6\mu_B^*$ which is even larger than the value expected for noninteracting electrons.²⁹ In agreement with this prediction we interpret our observation that ΔM is larger than the numerical result as a signature of electron-electron interaction.

Finally we take a view at the magnetization for $\nu < 2$ ($B > 10.5$ T in Fig. 3). In Fig. 13 a small linear slope (see Fig. 3) has been subtracted from the data between 10.5 and 14 T. At low temperature we find an oscillation at $B = 11.8$ T. This is in contrast to a noninteracting 2DES where the magnetization is expected to be constant in this regime. The position of the oscillation corresponds to the fractional quantum Hall state $\nu = 5/3$. The magnetization of fractional quantum Hall states has been studied in detail by Meinel *et al.* in very high mobility samples.⁴

VII. CONCLUSION

We have studied the magnetization of a 2DES over a large range of external parameters. In particular the high experimental accuracy of the MCM technique in the low-field regime has been important to access quantum numbers as large as $\nu = 40$ and to investigate the effect of disorder. Here the ground-state properties of the 2DES were dominated by the

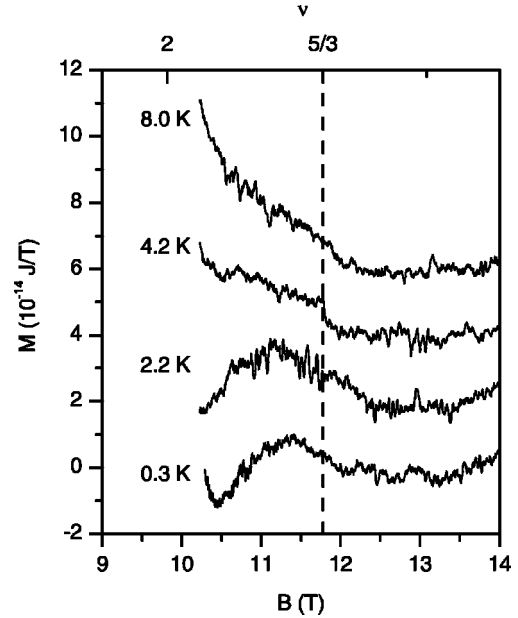


FIG. 13. Magnetization for $\nu < 2$. A linear decrease has been subtracted in order to visualize the structure at $\nu = 5/3$.

single-particle energies. The dependence of the DOS between the Landau levels on the filling factor could be qualitatively explained by the presence of edge states. Here further insight will be achieved by the investigation of smaller 2DES, where a stronger contribution of the edge states to the total magnetization can be expected. At high magnetic fields the limit of only one occupied Landau level was reached. With increasing field, i.e., decreasing quantum number ν , the electron-electron interaction gradually gains importance which is best seen from the enhancement of spin splitting by the Coulomb-exchange interaction.

ACKNOWLEDGMENTS

We acknowledge financial support from the Deutsche Forschungsgemeinschaft via SFB 508 and the projects He 1938/10-1 and Gr 1640/1-1 in the ‘‘Schwerpunktprogramm Quanten-Hall Systeme.’’

¹H.L. Stormer, T. Haavasoja, V. Narayanamurti, A.C. Gossard, and W. Wiegmann, *J. Vac. Sci. Technol. B* **2**, 423 (1983).

²J.P. Eisenstein, H.L. Stormer, V. Narayanamurti, A.Y. Cho, A.C. Gossard, and C.W. Tu, *Phys. Rev. Lett.* **55**, 875 (1985).

³S.A.J. Wieggers, M. Specht, L.P. Lévy, M.Y. Simmons, D.A. Ritchie, A. Cavanna, B. Etienne, G. Martinez, and P. Wyder, *Phys. Rev. Lett.* **79**, 3238 (1997).

⁴I. Meinel, T. Hengstmann, D. Grundler, D. Heitmann, W. Wegscheider, and M. Bichler, *Phys. Rev. Lett.* **82**, 819 (1999).

⁵I. Meinel, D. Grundler, D. Heitmann, A. Manolescu, V. Gudmundsson, W. Wegscheider, and M. Bichler, *Phys. Rev. B* **64**, 121306 (2001).

⁶E. Gornik, R. Lassnig, G. Strasser, H.L. Stormer, A.C. Gossard,

and W. Wiegmann, *Phys. Rev. Lett.* **54**, 1820 (1985).

⁷M.P. Schwarz, D. Grundler, I. Meinel, Ch. Heyn, and D. Heitmann, *Appl. Phys. Lett.* **76**, 3564 (2000).

⁸C.L. Jones, A. Usher, M. Elliott, W.G. Herrenden-Harker, A. Potts, R. Shepherd, T.S. Cheng, and C.T. Foxon, *Solid State Commun.* **95**, 409 (1995).

⁹J.P. Watts, A. Usher, A.J. Matthews, M. Zhu, M. Elliott, W.G. Herrenden-Harker, P.R. Morris, M.Y. Simmons, and D.A. Ritchie, *Phys. Rev. Lett.* **81**, 4220 (1998).

¹⁰D. Shoenberg, *Magnetic Oscillations in Metals* (Cambridge University Press, Cambridge, England, 1984).

¹¹T. Englert, D.C. Tsui, A.C. Gossard, and C. Uihlein, *Surf. Sci.* **133**, 295 (1982).

- ¹²R.R. Gerhardts and V. Gudmundsson, Phys. Rev. B **34**, 2999 (1986).
- ¹³V. Gudmundsson and R.R. Gerhardts, Phys. Rev. B **35**, 8005 (1987).
- ¹⁴V. Sa-yakanit, N. Choosiri, and H.R. Glyde, Phys. Rev. B **38**, 1340 (1988).
- ¹⁵L. Spies, W. Apel, and B. Kramer, Phys. Rev. B **55**, 4057 (1997).
- ¹⁶M.A. Itskovsky, T. Maniv, and I.D. Vagner, Phys. Rev. B **61**, 14 616 (2000).
- ¹⁷B.I. Halperin, Phys. Rev. B **25**, 2185 (1982).
- ¹⁸U. Sivan and Y. Imry, Phys. Rev. Lett. **61**, 1001 (1988).
- ¹⁹M.M. Fogler, E.I. Levin, and B.I. Shklovskii, Phys. Rev. B **49**, 13 767 (1994).
- ²⁰D.B. Chklovskii, B.I. Shklovskii, and L.I. Glazman, Phys. Rev. B **46**, 4026 (1992).
- ²¹M.R. Geller and G. Vignale, Phys. Rev. B **52**, 14 137 (1995).
- ²²L. Bremme, T. Ihn, and K. Ensslin, Phys. Rev. B **59**, 7305 (1999).
- ²³P. Weitz, E. Ahlswede, J. Weis, K.v. Klitzing, and K. Eberl, Physica E (Amsterdam) **6**, 247 (2000).
- ²⁴T. Ando and Y. Uemura, J. Phys. Soc. Jpn. **36**, 959 (1974).
- ²⁵R.R. Gerhardts, Z. Phys. B **21**, 275 (1975); Surf. Sci. **58**, 234 (1976).
- ²⁶K. Broderix, N. Heldt, and H. Leschke, Phys. Rev. B **40**, 7479 (1989).
- ²⁷T. Ando and Y. Uemura, J. Phys. Soc. Jpn. **37**, 1044 (1974).
- ²⁸C. Kallin and B.I. Halperin, Phys. Rev. B **30**, 5655 (1984).
- ²⁹A.H. MacDonald, H.C.A. Oji, and K.L. Liu, Phys. Rev. B **34**, 2681 (1986).